AN EXPERIMENTAL METHOD TO DETERMINE THE LONGITUDINAL INTRALAMINAR FRACTURE TOUGHNESS OF HIGH TENSILE STRENGTH FIBRE-REINFORCED UNIDIRECTIONAL COMPOSITES

Haibao Liu[1], Brian G. Falzon[1*], Wei Tan[1]

[1]School of Mechanical and Aerospace Engineering, Queen`s University Belfast, Ashby Building, Belfast, UK

Email: hliu07@qub.ac.uk, Web Page: http://www.qub.ac.uk/mechaero

Email: b.falzon@qub.ac.uk, Web Page: http://www.qub.ac.uk/mechaero

Email: wtan05@qub.ac.uk, Web Page: http://www.qub.ac.uk/mechaero

Keywords: High strength fibre, fracture toughness, elongation, non-distructive inspection

Abstract

The high tensile strength of a variety of commercially-available carbon fibres presents a considerable challenge in determining the fibre-dominated longitudinal intralaminar tensile fracture toughness of cured unidirectional composite plies. The use of standard compact tension specimens leads to premature buckling and crushing at the unloaded end of the specimen. A non-standardized grooved Compact Tension (CT) specimen as well as an external fixture was developed to limit these damage zones and promote crack propagation from the precrack location. Nonetheless, problems were still encountered with extensive sublaminate delamination followed by fibre extension and pull-out leading to fibre fracture. This made it difficult to measure the crack length. To mitigate this shortcoming, a novel measurement technique based on the fibre's elongation and non-destructuve inspection (NDI) was developed to determine an accurate crack length. An IMS60/epoxy composite system was used to manufacture cross-ply specimens $[(90/0)_s]_4$. Two different data reduction schemes, compliance calibration and the area method, were used to determine the fibre-dominated initiation and propagation fracture toughness values. Propagation values of fracture toughness were measured at 774.9 kJ/m^2 (compliance calibration) and 768.5 kJ/m^2 (area method), respectively. A computational model with an in-house VUMAT subroutine for ABAQUS/Explicit was developed to assess the accuracy of the measured fracture toughness. Good agreement was obtained between numerical and experimental results.

1. Introduction

Failure modes of composite materials are broadly classified as interlaminar and intralaminar failure. Interlaminar failure has been studied extensively and standard test and data reduction methods have been established. The double-cantilever beam (DCB) test and the end-notched flexure (ENF) test have been developed for mode I and mode II, respectively. Based on the DCB and ENF tests, the mixed-mode bending (MMB) test has been widely used for mixed-mode delamination testing. Collectively, these test methods are now part of the ASTM suite of standard test methods. [1–3]. There is still no agreed standard for intralaminar fracture toughness testing of composite plies. The accurate measurement of intralaminar fracture toughness associated with fibre-dominated tensile failure is more challenging than measuring interlaminar fracture toughness.

Excerpt from ISBN 978-3-00-053387-7

Some studies have been carried on the fracture toughness assoiated with fibre-dominated tensile failure. Vaidya and Sun studied the fracture characteristics of comppsite laminates and developed a fracture criterion which showed that the critical stress intensity factor for fibre failure is a material constant [4]. Blanco et al. investigated different geometric configurations of the compact tension (CT) specimen for the characterisation of the tensile intralaminar fracture toughness of woven composite laminates. Based on analysis, a design methodology was proposed for the design of an approperate compact tension specimen [5]. Donadon et al. proposed a methodology based on the numerical evaluation of the strain energy release rate, leading to new geometric correction functions for determining the geometry of non-standardized Overheight Compact Tension (OCT) specimens[6].

It is necessary to point out that the reference CT test was originally designed for isotropic materials, and the determination of fracture toughness relies on the accuracy of the measured crack length. Moreover, the basic requirement of the various proposed derivative testing methods for composite laminates, is that a crack can be made to propagate along the central cross-section of these cross-ply test samples[7,8], fracturing fibres aligned longitudinally (i.e. parallel to the loading direction). The particular mechanical properties of laminated composites such as good performance in tension and poor performance in shear and compression may lead to unexpected failure prior to the desired crack growth which presents a considerable challenge in the determination of ply-level tensile fracture toughness . Generally, the crack growth is optically monitored by a digital cramera which assumes that fibre-dominated crack growth is synchronous with visible crack growth. The new generation of high strength fibre reinforced composite materials presents some new difficulties to the intralaminar fracture toughness characterisation. Their excellent performance in tension leads to compression failure at the back end of the compact tension specimens and the high strength fibre makes the pull-out phenomenon become more apparent which can affect the accurate measurement of crack length [9].

In the present work, an external fixture was developed, using computational analysis, to prevent the appearance of unexpected failure prior to crack growth in the CT specimens. Grooves on either side of the CT specimen were used to investigate the fracture toughness of composite materials associated with fibre-dominated tensile failure. A new crack tracking method based on fibre elongation and NDI is proposed. The determination of the fibre-dominated fracture toughness was achieved using the compliance calibration method and area method, respectively. Additionally the measured fracture toughness value was used in a FE model of the test specimen, with an in-house VUMAT composites damage subroutine to verify the experimental approach. Good correlation between physical tests and numerical results was obtained.

2. Material and Manufacture

The material system used in this work is an IMS60/epoxy unidirectional carbon fibre/epoxy laminated composite. The specimens had a cross-ply symmetric lay-up $[(90/0)_s]_4$ and were manufactured using Resin Transfer Moulding (RTM). A flow distribution medium was used on the upper and lower surfaces of the preform to ensure complete wetting. To ensure the quality of the specimens, all panels were subsequently inspected using an ultrasonic NDI system to make sure the pristine specimens were free of any major defect.

The mechanical properties of a single composite ply were measured using standard test methods and are shown in Table 1.

Table 1. Mechanical properties of IMS60/epoxy

Property	Modulus(GPa)	Poisson`s ratio	Strength(MPa)
Value	$E_{11} = 152$; $E_{22} = E_{33} = 8.71$; $G_{11} = G_{22} = G_{33} = 4.14$	$\nu_{12} = \nu_{13} = 0.3$; $\nu_{23} = 0.33$	$X^T = 1930$; $X^C = 968$; $Y^T = 41.4$; $Y^C = 276$; $S_{12} = 82.1$

3. Specimen Configuration

Specimens were cut from larger panels produced using RTM. A band saw and a razor saw were used to machine the profile of the specimen and introduce the pre-crack, respectively. A groove was machined using a milling cutter along the pre-crack direction. The dimensions of the specimen is shown in Fig. 1.

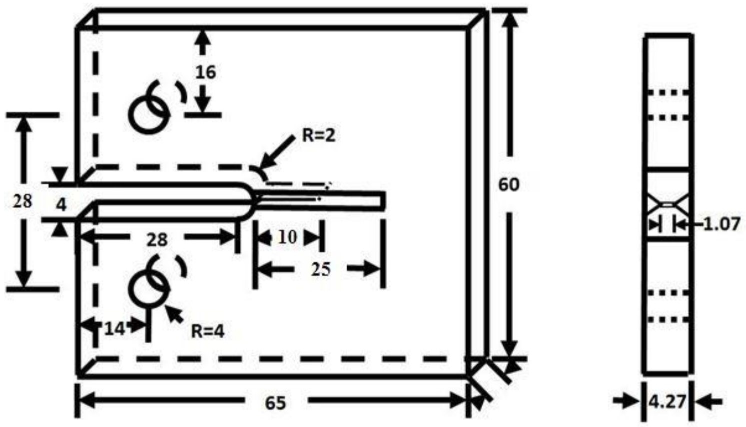

Figure 1. Dimensions of GCT specimen (all dimensions are in mm)

4. Experimental Setup

It is desired to have all damage in the specimen, resulting from a crack, propagating from the pre-crack, perpendicular to the loading direction and fracturing the longitudinal fibres in the process. Each specimen used in this work was manufactured from high-strength fibre which resulted in high strain energies developed within the specimen and causing damage in the back, upper and lower edges as shown in Fig. 2 (a). In order to obtain the proper failure mode at the mid-section, an external fixture was developed to prevent the damage at these susceptible regions. The fixture consists of two attachment types, the first to prevent back edge damage and the second to avoid upper and lower edges damage. The external fixture is shown in Fig. 2 (b).

The CT tests were carried out on the Houndsfield testing machine with a 50 KN load cell, under displacement control and at a loading rate of 1 mm/min. In order to capture the accurate displacement of the crack front point, Digital Image Correlation (DIC) was used to monitor the global strain distribution and to try and track the crack front. The time interval of the DIC frame capture was set at one second. Intervals were also marked on the top edge of the grooved area, and a digital camera was used to track the visible crack propagation. The experimental set-up is shown in Fig. 3 (a).

Excerpt from ISBN 978-3-00-053387-7

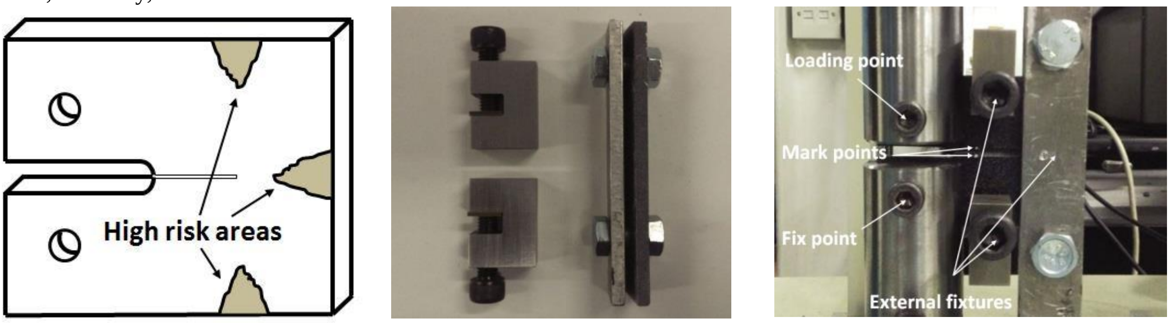

(a) (b) (c)

Figure 2. a) Susceptible regions b) external fixtures and c) assembly of specimen and fixtures.

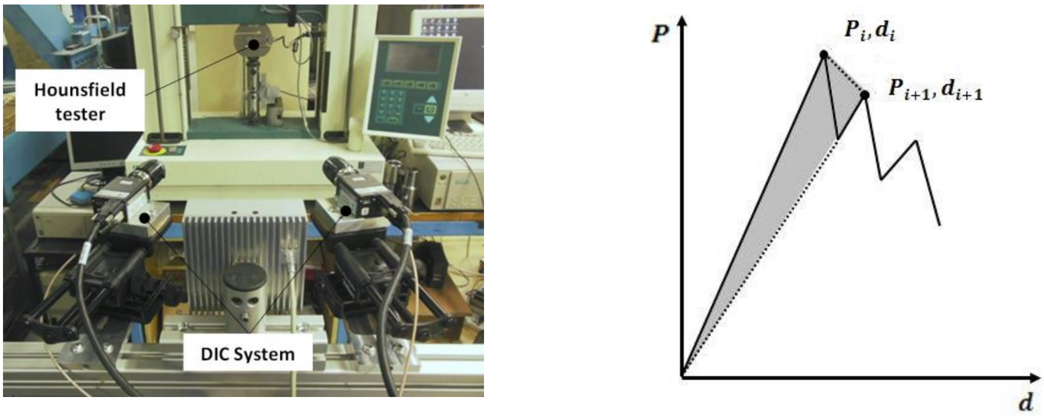

a) b)

Figure 3. Photographs of a) experiment set-up b) The definition of the area method

5. Data Reduction

So far, there are no specific test standards and data reduction schemes for the intralaminar fracture toughness characterisation of laminated continuous fibre composite materials [10]. A widely used data reduction method is the compliance calibration method. In this method, the critical strain energy release rate can be calculated using the change in compliance, C, with crack length,

$$G_{Ic}^{lam} = \frac{P_c^2}{2t}\frac{dC}{da} \tag{1}$$

Where P_c is the critical loading, at a given crack length, obtained from the load-displacement curve, C is compliance and a is the crack length. The experimental C versus a data was plotted and fitted with the function shown as Eq. 2,

$$C = (ma_v + n)^{\eta} \tag{2}$$

The values of m, n and η were calculated to best fit the experimental C versus a data. The critical strain energy release rate at each measured load was obtained from Eq. 3,

$$G_{Ic}^{lam} = \frac{P_c^2}{2t} m\eta(ma + n)^{\eta - 1} \tag{3}$$

Excerpt from ISBN 978-3-00-053387-7

For comparison, the area method data reduction scheme was also applied to compare these data reduction schemes. In this instance, the critical strain energy release rate can be calculated as

$$G_{Ic}^{lam} = \frac{1}{2t\Delta a}(P_i d_{i+1} - P_{i+1} d_i) \tag{4}$$

Where the critical loads, P_i, and respective displacement, d_i, are defined in the load-displacement plot shown in Fig. 3 (b). The shadow area indicates the energy dissipated in the creation of the corresponding fracture surface which was determined by the crack growth Δa.

Both data reduction schemes mentioned above require the measurement of crack length. Generally, the outermost layer of the compact tension specimen is a 90 degree ply which is perpendicular to the loading direction, so the optically measured crack length is the matrix crack length. In the compact tension test with lower strength fibre reinforced materials, the fibre breakage and matrix cracking are synchronous, so the visible crack length and fibre breakage length can be assumed to be the same. However, this assumption is not applicable to high strength fibre reinforced composites. The reason is that high strength fibre reinforced composites present significant fibre pull-out phenomenon which results in the fibre breakage 'lagging' behind the visible cracking as shown in Fig. 4(a). The crack shown in Fig. 4(b) appeared during the initial (rising) phase of the load-displacement curve, which suggests that the fibres are within their elastic response and undamaged, while, the optically measured crack length was 3 mm. This observation suggests that the fibre breakage and visible matrix cracking are not synchronous and the fibre breakage lags behind visible cracking.

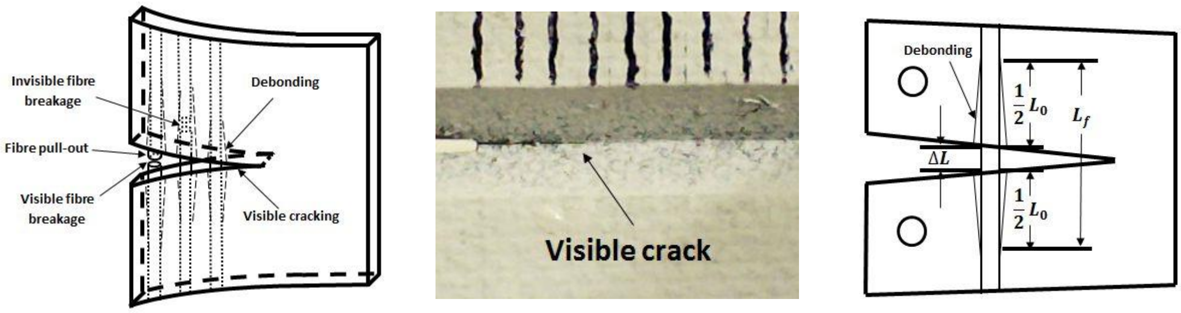

a) b) c)

Figure 4. a) high risk regions and b) visible cracking c) definition of localized linear strain

If the visible crack length was taken as the actual crack length, the measured fracture toughness value will be lower than the actual value. In order to determine the fibre-dominated tensile intralaminar fracture toughness, it is necessary to measure the accurate location of the crack tip corresponding to fibre-dominated fracture.

In this work, a novel but simple method for measuring the actual crack length in high strength fibre reinforced material was developed based on the fibre elongation and NDI technique. We define a localized linear strain, ε, as the ratio of extension, ΔL, to the initial length of the debonded fibre, L_0 (prior to crack opening), as shown in Fig 4 (c),

$$\varepsilon = \frac{\Delta L}{L_0} \tag{5}$$

Excerpt from ISBN 978-3-00-053387-7

When the CT test was completed and the specimen unloaded to its original position, the ultrasonic scan system shown in Fig. 5 (a) was used to capture the fibre debonding region of the tested specimen. A typical debonding area of the tested CT specimens is shown in Fig. 5 (b), The height of the debonging area (blue area) in the NDI map equals the initial length of the debonded fibre, L_0.

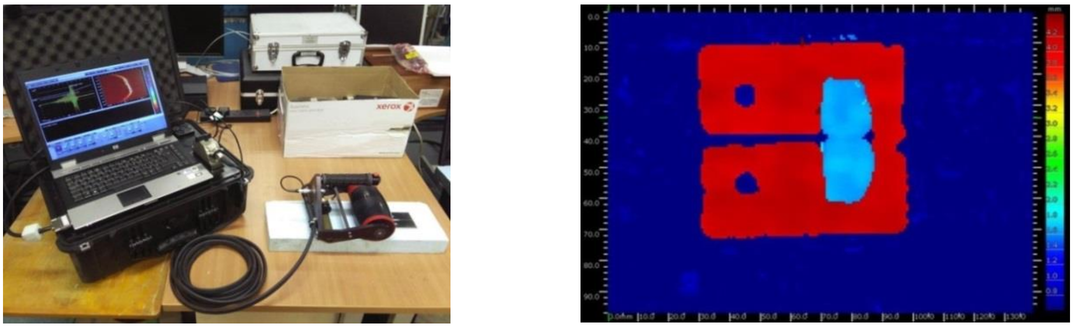

a) b)

Figure 5. a) Ultrasonic scan system b) measured debonding area

Based on the measured initial length of the debonded fibre and the maximum failure strain (obtained from tensile coupon tests), the maximum elongation at fracture is therefore the product of the failure strain, ε_f , and the initial length of the debonded fibre, Eq. 6,

$$\Delta L_{max} = L_0 \varepsilon_f \tag{6}$$

Once the maximum elongation, at the respective debonded region was determined, this value was used to compare with the visible crack opening at the corresponding region which reflects the fibre elongation. When visible crack opening was equivalent to the maximum elongation, the fibre in this region was deemed to have fractured, and this point was considered as the new crack tip. Finally, the crack length a was determined as the length from the loading point to this crack tip.

6. Results

The region in blue represents debonding in the CT specimens. The initial length was measured at 39 ± 1 mm. Based on coupon tensile tests, the fibre failure strain was measured at 1.9%, so the maximum elongation was determined to be 0.74± 0.02 mm. As shown in Fig. 6 (a), when the crack opening reached 0.74 mm, the fibres corresponding to this point were deemed to have fractured and the crack length, a, defined as AB. The measured compliance, based on the load-displacement curve, is shown in Fig. 6 (b).

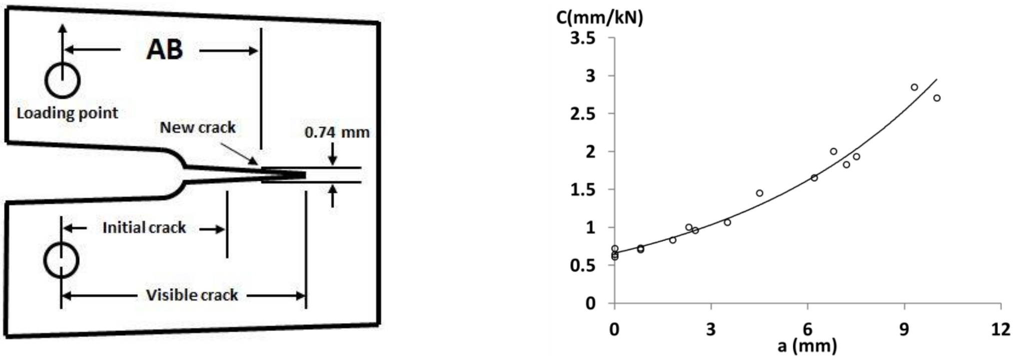

a) b)

Figure 6. a) Determination of crack tip b) Compliance versus crack length

The fibre breakage length at critical points was determined using the proposed novel measurement method with the assistance of NDI. Two different data reduction methods mentioned above, the area method and compliance calibration, were used to calculate the fibre-dominated tensile fracture toughness. The R-curves obtained using these two different methods of data reduction are shown in Fig. 7 (a) and (b).

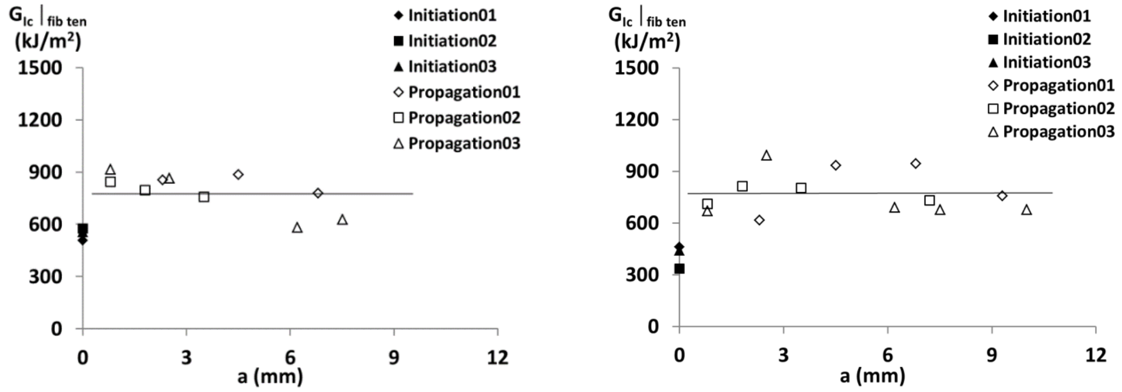

Figure 7. R-curve obtained from a) Area method and b) Compliance calibration

The initiation value of fracture toughness was defined as the toughness value calculated at data point $a = 0$, and the propagation value was defined as the average value of all toughness values obtained from data points for $a > 0$. A comparison of the measured initiation and propagation values of fracture toughness based on visible crack tracking and fibre elongation are shown in Table 2.

Table 2. Comparison of initiation and propagation values of fracture toughness (kJ/m^2)

Data reduction scheme	Area method	Compliance calibration
Initiation	546.1± 7.3%	413.1± 18.9%
Propagation	768.5± 4.1%	774.9 ± 5.2%

7. FE Simulation

As shown in Fig. 8 (a), a finite element model incorporating an in-house VUMAT composite damage subroutine for ABAQUS/Explicit was developed to assess the accuracy of the measured fracture toughness [11,12]. The crack front of the model was meshed with 0.4mm×0.2mm×0.13mm C3D8R elements with two elements through the thickness of each ply of the laminates.The general contact algorithm and cohesive surface available in ABAQUS/Explicit was used to simulate the globel contact of the model and the local contact between plies, respectively. A measured friction coefficient of 0.25 was employed for the ply-to-ply contact. As shown in Fig. 8 (b), the simulation results were in good agreement with the physical test results.

Excerpt from ISBN 978-3-00-053387-7

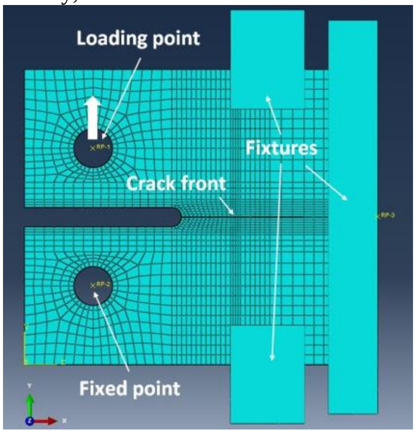

a)

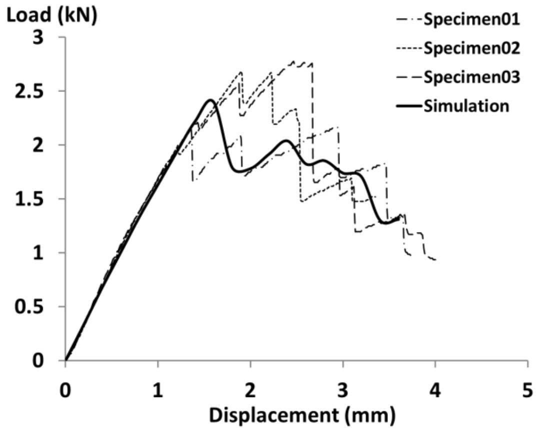

b)

Figure 8. a) FE model and b) Load-diaplacement curves from simulation and experiment

8. Conclusions

In this work, an external fixture was designed, guided by stress analysis, to eliminate the risk of compressive damage in CT specimen regions remote from the desired crack path. The accurate crack lengths at corresponding critical loads were determined using a novel crack length measurement methodology which combined fibre elongation information and an ultrasonic NDI technique. Two different data reduction schemes, the area method and compliance calibration method, were used to assess the accuracy of the tensile fracture toughness values of an IMS60/epoxy composite ply. The propagation values of toughness calculated by both data reduction methods were consistent. The initiation values obtained from the area method were higher than those from the compliance calibration method. The numerical results delivered by the FE model with measured propagation values of fracture toughness obtained very good correlation with experimental results.

9. Acknowledgement

The authors would like to acknowledge the financial support of Bombardier and the Royal Academy of Engineering. The authors are also indebted to Mr Dave Thompson from the Northern Ireland Advanced Composites and Engineering Centre (NIACE) / BAB Strategic Technology for his discussions and suggestions.

References

[1] ASTM D5528-01. Standard Test Method for Mode I Interlaminar Fracture Toughness of Unidirectional Fiber-Reinforced Polymer Matrix Composites, 2004.
[2] ASTM D7905/D7905M-14. Standard Test Method for Determination of the Mode II Interlaminar Fracture Toughness of Unidirectional Fiber-Reinforced Polymer Matrix Composites: 1–18, 2004.
[3] ASTM D6671/D6671M-03. Standard Test Method for Mixed Mode I-Mode II Interlaminar Fracture Toughness of Unidirectional Fiber Reinforced Polymer Matrix Composites, 2004.
[4] ZP Bažant, IM Daniel, and Z Li. Size effect and fracture characteristics of composite laminates. *Journal of Engineering Materials and Technology*, 118: 317–24, 1996.
[5] N Blanco, D Trias, ST Pinho, and P Robinson. Intralaminar fracture toughness characterisation of woven composite laminates . Part I : Design and analysis of a compact tension (CT) specimen. *Engineering Fracture Mechanics*, 131: 349–60, 2014.
[6] M V Donadon, BG Falzon, L Iannucci, and JM Hodgkinson. Measurement of Fibre Fracture Toughness Using an Alternative Specimen Geometry. *Proceedings of the16th International*

Excerpt from ISBN 978-3-00-053387-7

Conference on Composite Materials ICCM-16, Kyoto, Japan, July 8-13, 2007.

[7] ST Pinho, P Robinson, and L Iannucci. Fracture toughness of the tensile and compressive fibre failure modes in laminated composites. *Composites Science and Technology*, 66: 2069–79, 2006.

[8] MJ Laffan, ST Pinho, P Robinson, L Iannucci, and a. J McMillan. Measurement of the fracture toughness associated with the longitudinal fibre compressive failure mode of laminated composites. *Composites Part A: Applied Science and Manufacturing*, 43: 1930–8, 2012.

[9] AC Bergan, and CG Dávila. Cohesive Laws for Analyzing Through-Crack Propagation in Cross Ply Laminates. *Proceedings of the 20th International Conference on Composite Materials ICCM-20, Copenhagen, Denmark*, July 19-24, 2015.

[10] M V. Donadon, BG Falzon, L Iannucci, and JM Hodgkinson. Intralaminar toughness characterisation of unbalanced hybrid plain weave laminates. *Composites Part A: Applied Science and Manufacturing*, 38: 1597–611, 2007.

[11] BG Falzon, and P Apruzzese. Numerical analysis of intralaminar failure mechanisms in composite structures. Part I: FE implementation. *Composite Structures*, 93: 1039–46, 2011.

[12] BG Falzon, and P Apruzzese. Numerical analysis of intralaminar failure mechanisms in composite structures. Part II: Applications. *Composite Structures*, 93: 1039–46, 2011.

Excerpt from ISBN 978-3-00-053387-7